

# Efficient Implementation of Complex Particle Shapes in the Lattice Solid Model

Steffen Abe and Peter Mora

ACcESS

The University of Queensland  
St Lucia, QLD 4072, Australia

(steffen@quakes.uq.edu.au, mora@quakes.uq.edu.au)

**Abstract.** The lattice solid model is a particle based simulation model for the study of earthquake micro-physics and rock mechanics. It consists of particles interacting by various types of mechanisms such as elastic-brittle forces and friction. Results of laboratory experiments have shown that the grain shape has a major influence on the frictional properties of fault gouge. In order to enable realistic simulations it is thus important to include the capability to model non-spherical particles into the simulation software. To achieve this goal a new class of particles with variable shapes have been implemented in the lattice solid model. The shape of the particles is described by an arbitrary number of piecewise spherical patches. This leads to a good balance between the computational cost of the contact detection and calculation of interactions between particles and the range of particle shapes available.

## 1 Introduction

The lattice solid model (Mora and Place, 1994 [10], Place and Mora, 1999 [13]) is a particle based simulation model for the study of earthquake micro-physics and rock mechanics similar to the discrete element model (Cundall and Strack, 1979 [3]). It consists of particles interacting by various types of mechanisms such as brittle-elastic forces and friction. Results of laboratory experiments comparing the frictional behavior of fault gouge consisting of spherical grains with a gouge containing angular grains (Mair et al., 2002 [9]) have shown that grain shape has a major influence on the frictional properties of granular gouge. In order to enable realistic simulations it is thus important to include the capability to model non-spherical particles into the simulation software.

Place and Mora, 2000 [14] have successfully used strongly bonded groups of spherical particles to model angular grains in a 2D simulation of shear of a granular fault gouge. A similar approach has been used by Pöschel and Buchholtz, 1993 [15] and Mahboubi et al., 1997 [8] using aggregates of variable sized spheres. While enabling the simulation of arbitrarily shaped grains in a simple and efficient way, the surface roughness of the grains is determined by the size of the spherical particles used to construct the grain. Thus grains formed by a low number of particles will always have a high surface roughness and

the modeling of grains with low surface roughness requires the grains to be constructed from a large number of spherical particles and thus leads to high computational cost.

Other approaches for the modeling of non-spherical grains in DEM simulations include elliptical or super-ellipsoidal particles (Ting et al., 1993 [17], Mustoe and DePoorter, 1993 [12], Cleary et al., 1997 [2]), polyhedra (Cundall, 1988 [4], Hogue and Newland, 1993 [6], Hogue and Newland, 1994 [7]) and discrete function representation (Williams and O'Connor, 1995 [18], Hogue, 1998 [5]). The use of elliptical or super-ellipsoidal particles strongly restricts the types of grain shapes which can be modeled, in particular with respect to the symmetry of the grains. While polyhedra and discrete function representations allow arbitrary shapes, a good approximation of smooth grain shapes requires a large number of vertices, leading to computationally expensive contact detection algorithms.

In order to achieve a balance between a high flexibility in the choice of grain shapes and computational efficiency a new class of grain shape representations for the use in lattice solid or DEM simulation has been developed based on grains constructed from overlapping spherical patches. Each grain consists of an arbitrary number of sphere segments forming the surface of the grain (Figure 1). The positions and orientations of the spherical patches are fixed relative to each other. A somewhat similar approach using overlapping spheres to construct non-spherical particles has been presented by Zhang and Vu-Quoc [19], however they used only four identical full spheres whereas the approach presented here uses an arbitrary number of spherical patches.

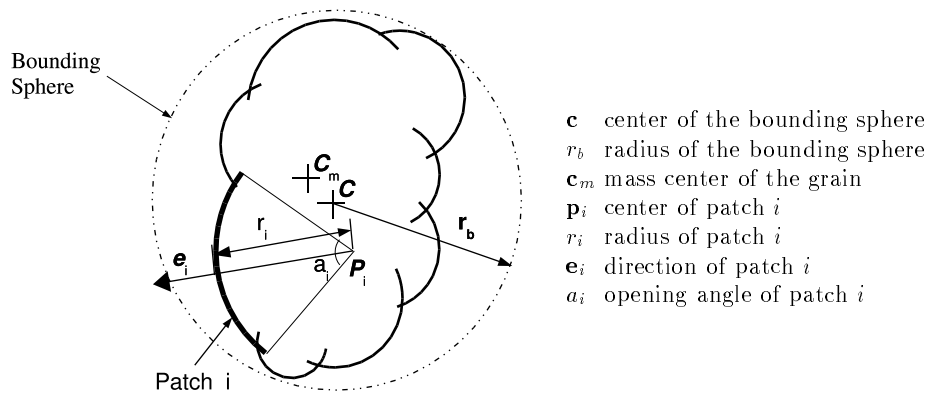


**Fig. 1.** Structure of a grain constructed from overlapping spherical patches. The figure is drawn in 2D for simplicity but the same structure applies to 3D particles.

The advantages of using spherical patches are that the detection of a contact between them can be implemented at a low computational cost (34Flops worst case) and that while arbitrary grain shapes can be constructed using a sufficient

number of patches, some particle shapes can be approximated by a very small number of patches. However, some classes of grain shapes, in particular those with large flat surfaces and sharp edges would require a large number of patches for a good approximation and may be more efficiently simulated using other, for example polyhedral, approaches. The approach presented here is more suited to rounded grains.

## 2 The Algorithm

The Algorithm for the calculation of the motion of the grains can be separated into two parts: detection of the contacts between the grains including the calculation of the contact parameters and the calculation of the contact forces and the resulting grain movement.

### 2.1 Contact Detection

As a first step to find contact between two grains  $k$  and  $l$  the intersection between the bounding spheres of the grains is tested. If the bounding spheres intersect, i.e if the distance between their centers  $\mathbf{c}_k$  and  $\mathbf{c}_l$  is smaller than the sum of the radii  $r_k$  and  $r_l$

$$|\mathbf{c}_k - \mathbf{c}_l| < r_k + r_l \quad , \quad (1)$$

contact between the two grains is possible. If the bounding spheres do not intersect, the contact detection algorithm for the pair of grain terminates and the next pair of grains is considered.

If the bounding spheres intersect, each pair of spherical patches  $i$  and  $j$  contained in grains  $k$  and  $l$  respectively is tested for intersection. This test is performed in two steps. First the distance between the patch centers  $\mathbf{p}_i$  and  $\mathbf{p}_j$  is compared with the sum of the patch radii  $r_i$  and  $r_j$ . If the distance between the patch centers is small enough, i.e.

$$|\mathbf{p}_i - \mathbf{p}_j| < r_i + r_j \quad . \quad (2)$$

it is then tested if the direction  $\mathbf{e}_{ij}^d$ , which connects the patch centers is within both patches. If the distance is too large no contact between the patches is possible and the next pair of patches is considered.

The direction of the vector  $\mathbf{e}_{ij}^d$  between the patch centers can be calculated as

$$\mathbf{e}_{ij}^d = \frac{\mathbf{p}_i - \mathbf{p}_j}{|\mathbf{p}_i - \mathbf{p}_j|} \quad . \quad (3)$$

The direction  $\mathbf{e}_{ij}^d$  is within a patch  $i$  if the angle between  $\mathbf{e}_{ij}^d$  and the direction  $\mathbf{e}_i$  is smaller than the bounding angle  $\alpha_i$  of the patch  $i$ . Thus if the conditions

$$\mathbf{e}_{ij}^d \cdot \mathbf{e}_i < \cos \alpha_i \quad (4)$$

$$-\mathbf{e}_{ij}^d \cdot \mathbf{e}_j < \cos \alpha_j \quad (5)$$

are both fulfilled, a contact between the patches  $i$  and  $j$  has been found. The actual contact point is assumed to be in the center of the overlapping region between the patches along the line connecting the patch centers (Figure 2). The location  $x_{ij}$  of the contact can thus be computed as

$$\begin{aligned} \mathbf{x}_{ij} &= \mathbf{p}_i + \mathbf{e}_{ij}^d \left( \frac{\mathbf{p}_i - \mathbf{p}_j}{r_i + r_j} \right) \\ &= \mathbf{p}_j - \mathbf{e}_{ij}^d \left( \frac{\mathbf{p}_j - \mathbf{p}_i}{r_i + r_j} \right) . \end{aligned} \quad (6)$$

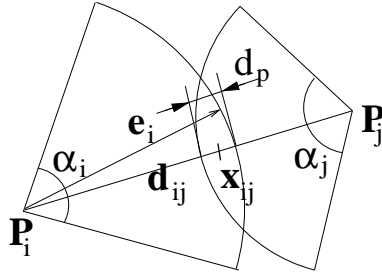


**Fig. 2.** Intersection between two patches. The figure is drawn in 2D for simplicity but the same structure applies to 3D particles. The point  $x_{ij}$  is the contact point assumed for force and motion calculations.

The contact normals  $\mathbf{n}_i$  and  $\mathbf{n}_j$  are assumed to be the surface normals of the patch at the contact point which, given that the patch surfaces are parts of spheres, can be calculated from the direction of the connecting line between the patch centers,

$$\mathbf{n}_i = \frac{\mathbf{d}_{ij}}{|\mathbf{d}_{ij}|} \quad (7)$$

$$\mathbf{n}_j = \frac{\mathbf{d}_{ji}}{|\mathbf{d}_{ji}|} = -\mathbf{n}_i \quad (8)$$

The penetration depth  $d_p$  (Figure 2) of the two patches at the contact point, which is needed for the subsequent calculation of the contact forces, can be calculated as the difference between the sum of the radii  $r_i$  and  $r_j$  and the distance between the patch centers  $\mathbf{p}_i$  and  $\mathbf{p}_j$

$$d_p = |(\mathbf{p}_i - \mathbf{p}_j)| - (r_i + r_j) \quad (9)$$

## 2.2 Calculation of Forces and Particle Motions

As a first step in the calculation of the motion of grains the contact forces are calculated from the contact parameters obtained by the contact detection

algorithm. In lattice solid and DEM simulations a wide variety of contact forces have been implemented, including linear elastic forces (Mora and Place, 1994 [10]), Hertz-Mindlin contact laws (Morgan and Boettcher, 1999 [11]) and both linear and nonlinear friction forces (Cundall, 1979 [3], Place and Mora, 1999 [13], Abe et al., 2002 [1]). All those contact forces can be implemented here in the same way because the locally spherical shape of the grains at the point of contact. The total force at each contact  $\mathbf{f}_{ij}$  can then be calculated as the sum of the forces due to each of the interactions at this contact

$$\mathbf{f}_{ij} = \mathbf{f}_{ij}^{elast} + \mathbf{f}_{ij}^{fric} + \dots \quad (10)$$

and the total force  $\mathbf{f}_{grain}$  on each grain can be calculated as the sum of all contact forces applied to this grain

$$\mathbf{f}_{grain} = \sum_{patches} \mathbf{f}_{ij} \quad (11)$$

The calculation of the particle motions follows the approach derived in (Shabana, 1994 [16]). The linear acceleration  $\mathbf{a}_i$  of grain  $i$  can be calculated directly from the total force  $\mathbf{f}_i$  applied to this grain

$$\mathbf{a}_i = \frac{\mathbf{f}_i}{m_i} \quad (12)$$

where  $m_i$  is the mass of grain  $i$ . The velocity  $\mathbf{v}_i$  and position  $\mathbf{x}_i$  of the grain can then be updated using an appropriate integration scheme. Currently a simple first order method is used:

$$\mathbf{v}_i(t + \Delta t) = \mathbf{v}_i(t) + \Delta t \mathbf{a}_i \quad (13)$$

$$\mathbf{x}_i(t + \Delta t) = \mathbf{x}_i(t) + \Delta t \mathbf{v}_i \quad (14)$$

For the grain rotation it is necessary to calculate the torque  $\tau_i$  applied to the grain from the contact forces  $\mathbf{f}_{ij}$  and the contact positions  $\mathbf{x}_{ij}$  relative to the center of mass  $\mathbf{c}_m$  of the grain

$$\tau_i = \sum_{patches} (\mathbf{x}_{ij} - \mathbf{c}_m) \times \mathbf{f}_{ij} \quad . \quad (15)$$

Using the torque the change in angular momentum can be calculated

$$\dot{\mathbf{l}}_i = \frac{\tau_i}{\mathbf{I}_i} \quad , \quad (16)$$

where  $\mathbf{I}_i$  is the inertia tensor of grain and from this the angular velocity  $\omega$  and orientation  $\mathbf{R}_i$  can be updated similar to the linear movement (Eq. 13)

$$\omega_i(t + \Delta t) = \omega_i(t) + \Delta t \dot{\mathbf{l}}_i \quad (17)$$

$$\mathbf{R}_i(t + \Delta t) = \mathbf{R}_i(t) + \omega \star \mathbf{R}_i \Delta t \quad (18)$$

After updating the position  $\mathbf{x}_i$  and orientation  $\mathbf{R}_i$  of the grain the positions of the patch centers  $\mathbf{p}_i$  and orientations  $\mathbf{e}_i$  need to be updated

$$\mathbf{p}_i^{new} - \mathbf{c}_m = \mathbf{R}_i(\mathbf{p}_i^0 - \mathbf{c}_m) \quad (19)$$

$$\mathbf{e}_i^{new} = \mathbf{R}_i \mathbf{e}_i^0 \quad , \quad (20)$$

where  $\mathbf{p}_i^0$  and  $\mathbf{e}_i^0$  are the initial values for the patch center positions and patch directions. Also, the inertia tensor  $\mathbf{I}_i^0$  of the grain needs to be updated

$$\mathbf{I}_i^{new} = \mathbf{R}_i \mathbf{I}_i^0 \mathbf{R}_i^T \quad . \quad (21)$$

Changes to the inertia tensor  $\mathbf{I}_i^0$  due to deformation of the grain are ignored.

### 3 Verification Test

In order to verify the correctness of the implementation of the complex particle shapes in the lattice solid model tests have been performed. If there is no energy input into a simulation model and no energy dissipated in the model, the total energy contained in the model should remain constant if the implementation is correct. While the conservation of energy is not proof of the correctness of the implementation, a violation of the conservation of energy would show that the implementation is incorrect. Thus the conservation of energy can provide a useful consistency check.

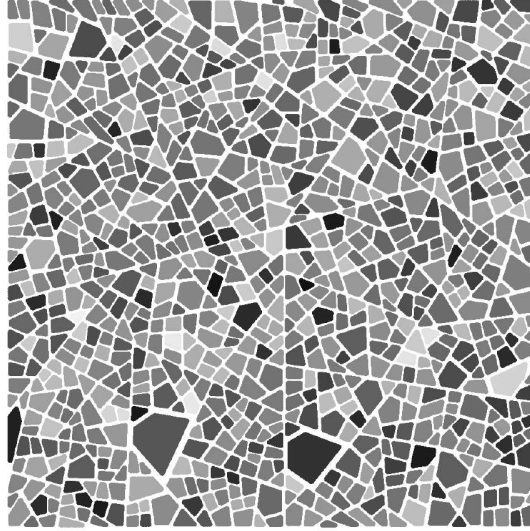


**Fig. 3.** Initial configuration of the model used for the verification test.

If the particles are interacting by elastic forces only, the only types of energy in the model are the kinetic energy of the grains  $E_{kin}$  and the elastic energy stored in the contacts between the grains  $E_{elastic}$ .

$$E_{total} = \sum_{particles} E_{kin}^i + \sum_{contacts} E_{elastic}^j \quad (22)$$

The kinetic energy of each grain  $E_{kin}^i$  can be calculated as the sum of translational part  $E_{trans}^i$  and a rotational part  $E_{rot}^i$

$$\begin{aligned} E_{kin}^i &= E_{trans}^i + E_{rot}^i \\ &= \frac{1}{2}m_i v^2 + \frac{1}{2}\omega_i \mathbf{I}_i \omega_i^T \quad . \end{aligned} \quad (23)$$

The elastic energy stored in a linear elastic contact  $j$  can be calculated from the spring constant  $k^j$  for the normal elastic interactions and the penetration depth  $d_p^j$  (Eq. 9)

$$E_{elastic}^j = \frac{1}{2}k^j(d_p^j)^2 \quad . \quad (24)$$

The elastic interactions between the spherical patches used in this model are the same as the elastic interactions used between the spherical particles in the original lattice solid model (Mora and Place, 1994 [10]).

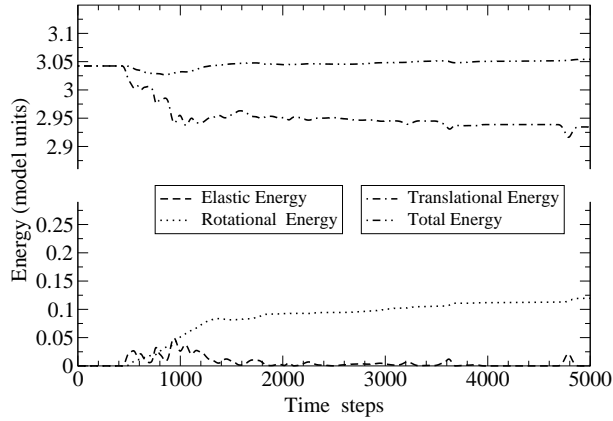


**Fig. 4.** Energy in the model during the simulation. The total energy is the sum of translational, rotational and elastic energy.

A 2D model is set up consisting of  $\approx 900$  random grains consisting of around 30 patches each (Figure 3) interacting only by linear elastic forces. The grains have been created by randomly splitting the model area into polygonal tiles and then generating each particle so that it best fits one of the tiles while maintaining

a prescribed minimum patch radius. The grains have a random initial linear velocity and no initial angular velocity.

The simulation is then run for 5000 time steps and the translational, rotational and elastic energy in the system are recorded. The total energy is then calculated according to Equation 22. The results (Figure 4) show that the total energy in the system remains constant within about 2.5%.

## 4 Conclusions

A new class of particles allowing the representation of arbitrary grain shapes based on composite grains constructed from spherical patches has been implemented in the lattice solid model. This will enable the more realistic simulation of processes in granular media which are sensitive to grain shape, such as the frictional behavior of fault gouge.

## Acknowledgments

This work was supported by the Australian Computational Earth Systems Simulator (ACcESS) Major National Research Facility.

## References

1. Abe, S., Dieterich, J.H., Mora, P., Place, D.: Simulation of the Influence of Rate and State dependent Friction on the Macroscopic Behavior of Complex Fault Zones with the Lattice Solid Model *Pure Appl. Geoph.*, 2002
2. Cleary, P.W., Stokes, N., Hurley, J.: Efficient Collision Detection of Three Dimensional Super-ellipsoidal Particles *Comp. Techniques and Applications*, 1997
3. Cundall, P. A., Strack, O. D. A.: A discrete numerical model for granular assemblies *Geotechnique* **29** 1979
4. Cundall, P. A.: Formulation of a Three-dimensional Distinct Element Model – Part I. A Scheme to Detect and Represent Contacts in a System Composed of Many Polyhedral Blocks *Int. J. Rock. Mech. Min. Sci. & Geomech. Abstr.* **25 No. 3** 1988
5. Hogue, C.: Shape Representations and Contact Detection for Discrete Element Simulations of Arbitrary Geometries *Engineering Computations* **15 No.3** 1998
6. Hogue, C., Newland, D.,: Efficient computer modelling of the motion of arbitrary grains in: *Powders and Grains 93*, Thornton (ed.), 1993
7. Hogue, C., Newland, D.,: Efficient computer simulation of moving granular particles *Powder Technology*, **78** 1994
8. Mahboubi, A., Cambrou, B., Fry, J.J.: Numerical modeling of the mechanical behavior of non-spherical, crushable particles in: *Powders and Grains 97*, Behringer and Jenkins (eds.) 1997
9. Mair, K., Frye, K.M., Marone, C.: Influence of Grain Characteristics on the Friction of Granular Shear Zones *J. Geophys. Res.* **107 B10** 2002
10. Mora, P., Place, D.: Simulation of the Stick-Slip Instability *Pure Appl. Geophys.* **143** (1994)

11. Morgan, J.K., Boettcher, M.S.: Numerical simulations of granular shear zones using the distinct element Method: 1. Shear zone kinematics and the micromechanics of localization *J. Geoph. Res.* **104 B2**, 1999
12. Mustoe, G.G.W., DePoorter, G.: A numerical model for the mechanical behavior of particulate media containing non-circular shaped particles in: *Powders and Grains 93*, Thornton (ed.), 1993
13. Place, D., Mora, P.: The Lattice Solid Model to Simulate the Physics of Rocks and Earthquakes: Incorporation of Friction *J. Comp. Phys.* **150** (1999)
14. Place, D., Mora, P.: Numerical Simulation of Localization Phenomena in a Fault Gouge *Pure Appl. Geophys.* **157** 2000
15. Pöschel, T., Buchholtz, V.: Static Friction Phenomena in Granular Materials: Coulomb Law versus Particle Geometry *Phys. Rev. Lett.* **71 n. 24** 1993
16. Shabana, A.A.: *Computational Dynamics* J. Wiley & Sons, 1994
17. Ting, J.M., Khwaja, M., Meachum, L.R., Rowell, J.D.: An Ellipse-Based Discrete Element Model For Granular Materials *Int. J. Num. Ana. Meth. Geomech.* **17** 1993
18. Williams, J. R., O'Connor, R. A Linear Complexity Intersection Algorithm for the Discrete Element Simulation of Arbitrary Geometries *Engineering Computations* **12** 1995
19. Zhang, X., Vu-Quoc, L.: Simulation of chute flow of soybeans using an improved tangential force-displacement model *Mechanics of Materials* **32**, 2000